

Accepted Manuscript

Discovery of novel bacterial FabH inhibitors (Pyrazol-Benzimidazole amide derivatives): Design, synthesis, bioassay, molecular docking and crystal structure determination

Yan-Ting Wang, Tian-Qi Shi, Jie Fu, Hai-Liang Zhu



PII: S0223-5234(19)30244-2

DOI: <https://doi.org/10.1016/j.ejmech.2019.03.026>

Reference: EJMECH 11196

To appear in: *European Journal of Medicinal Chemistry*

Received Date: 31 December 2018

Revised Date: 11 March 2019

Accepted Date: 11 March 2019

Please cite this article as: Y.-T. Wang, T.-Q. Shi, J. Fu, H.-L. Zhu, Discovery of novel bacterial FabH inhibitors (Pyrazol-Benzimidazole amide derivatives): Design, synthesis, bioassay, molecular docking and crystal structure determination, *European Journal of Medicinal Chemistry* (2019), doi: <https://doi.org/10.1016/j.ejmech.2019.03.026>.

This is a PDF file of an unedited manuscript that has been accepted for publication. As a service to our customers we are providing this early version of the manuscript. The manuscript will undergo copyediting, typesetting, and review of the resulting proof before it is published in its final form. Please note that during the production process errors may be discovered which could affect the content, and all legal disclaimers that apply to the journal pertain.

Abstract

The enzyme FabH catalyzes the initial step of fatty acid biosynthesis that is essential for bacterial survival. Therefore, FabH has been identified as an attractive target for the development of new antibacterial agents. We present here the discovery of a promising new series of Pyrazol-Benzimidazole amides with low toxicity and potent FabH inhibitory. Twenty-seven novel compounds have been synthesized, and all the compounds were characterized by $^1\text{H-NMR}$, $^{13}\text{C-NMR}$ and MS. Afterwards they were evaluated for *in-vitro* antibacterial activities against *E. coli*, *P. aeruginosa*, *B. subtilis* and *S. aureus*, along with *E. coli* FabH inhibition and cytotoxicity test. Some compounds proved to be of low toxicity and potent, especially compound **31** exhibited the most potential to be a new drug with MIC of 0.49-0.98 $\mu\text{g/mL}$ against the tested bacterial strains and IC_{50} of 1.22 μM against *E. coli* FabH. Eight analogues **16, 28, 30, 31, 33, 34, 35** and **36** with low range MIC against wild type *Xanthomonas Campestris* exhibited no inhibition against FabH-deficient mutant strain, which firmly proved the class of compounds arrived at antibacterial activity via interacting with FabH. *In silico* ADMET (Absorption, Distribution, Metabolism, Excretion and Toxicity) evaluation also pointed out that these compounds are potential for druggability. Further, effective overall docking scores of all the compounds have been recorded, and docking simulation of compound **31** into *E. coli* FabH binding pocket has been conducted, where solid binding interactions has been identified.

Keywords: FabH, Inhibitor, Pyrazole, Antibacterial, Molecule docking

1. Introduction

Although many kinds of antibacterial agents were discovered and used for clinical treatment, the incidences of drug resistance of microorganisms to antibacterial agents were constantly reported [1, 2]. Therefore, the development of new types of antibacterial agents is a very vital task and much of the research effort is oriented to the design of new antibacterial agents with high efficiency [3]. Recently, the research has been focused toward development of new antibacterial agents with novel target. A promising target is the fatty acid synthase (FAS) pathway in bacteria.

Bacterial FAS (type II) has been proved to be indispensable for bacteria cell survival [4, 5], which provides essential fatty acids for use in the assembly of key cellular components such as cell envelope, phospholipids, lipoproteins, lipopolysaccharides, and mycolic acids.

A key enzyme in this pathway is β -ketoacyl-acyl carrier protein synthase III (FabH) that initiates the fatty acid elongation cycles [6] and participates in the feedback regulation of FAS via product inhibition [7-9]. As shown in Fig. 1., FabH catalyzes the condensation reaction between a CoA-attached acetyl group and an ACP-attached malonyl group, yielding acetoacetyl-ACP as its final product [10]. In addition, FabH proteins are highly conserved at the sequence and structural level in both Gram-positive and -negative bacteria, while there are no significantly homologous proteins in humans. These attributes suggest that small molecule inhibitors of FabH enzymatic activity could be potential development candidates leading to selective, nontoxic, and broad-spectrum antibacterial [6].

The natural products platensimycin and platecin (Fig. 2.), discovered by employing a novel antisense differential sensitivity screening strategy, were reported recently from soil bacterial strains of *Streptomyces platensis* [11-13]. Platencin is considered a dual FabH-FabF inhibitor. The most potent of the natural products targeting the condensing enzymes is platensimycin, a nanomolar inhibitor of bacterial elongation condensing enzymes, which has a MIC of between 0.5-1.0 $\mu\text{g/ml}$ for several important pathogens, including *S. aureus*, *Enterococcus faecium*, and *Streptococcus pneumonia* [14, 15]. Compound **1** is a representative benzoic acid FabH inhibitor [16], which exhibits potent inhibitory activity against *Enterococcus faecalis* FabH and *Streptococcus pyogenes* FabH, $\text{IC}_{50} = 0.004\mu\text{mol/L}$.) FAS20013 is

an anti-tuberculosis drug developed by FASgen Company [17], which was originally designed with FabH as its target. It exerts potent inhibition against multi-drug resistant *Mycobacterium tuberculosis*, MIC = 0.75-1.5 mg/L.) as well as compounds **2** and **3**, discovered by McKinney et al. [18].

According to the structure analysis of these patent FabH inhibitors reported in the literatures, phenylamide is an important structural fragment, which can be used as the skeleton structure of new FabH inhibitors. Besides, with the aid of computer-aided drug design, Li screened a large number of compounds with different structures, and results also revealed that phenylamide fragment in drug was beneficial to FabH inhibition [19]. In addition, Subramani et al. exactly right exploited benzoyl amino benzoic acid (compound **4**) as the skeleton structure to design and develop novel drugs targeting FabH which exhibited potent activity [20].

Moreover, Polycyclic compounds containing benzimidazole ring units exhibit multiple excellent biological activities, including antibacterial, antifungal, anticancer, analgesic, anti-inflammatory, antioxidant antidiabetic, antiparasitic, antihypertensive ones and so on [21-26].

Further, Pyrazole possesses low molecular weight and steric hindrance, and is often contributed as an active structural fragment to antimicrobial design [27].

Yet, the effectiveness of fragment hybrid of phenyl amide, benzimidazole and pyrazole has not been studied till now. To address this knowledge gap, a series of novel Pyrazol-Benzimidazole amides targeting FabH was synthesized by fragment hybrid, then modification.

In this paper, some work has been done: discuss the synthetic method of this series of novel compounds, depict the results of reactivity studies; evaluate their antibacterial and anti-FabH activities; detect cytotoxicity and hemolytic activities; appraise *in silico* ADMET (Absorption, Distribution, Metabolism, Excretion, Toxicity). Additionally, molecular docking provided more information that could elucidate antimicrobial mechanisms.

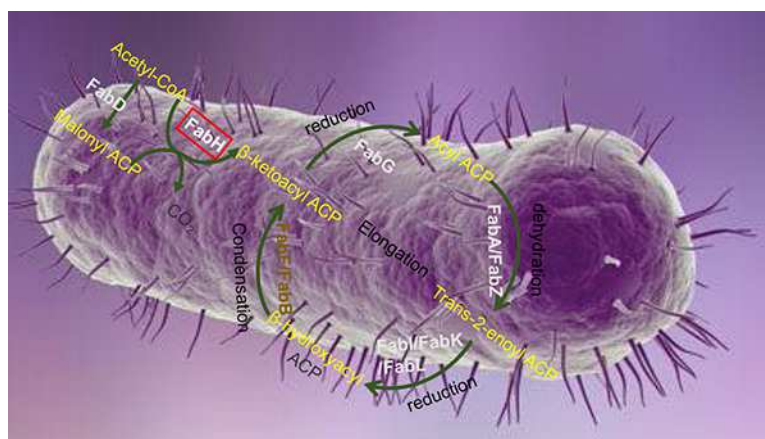


Fig. 1. Fatty acid biosynthesis pathway (FabH catalyzes the initiation reaction) [10]

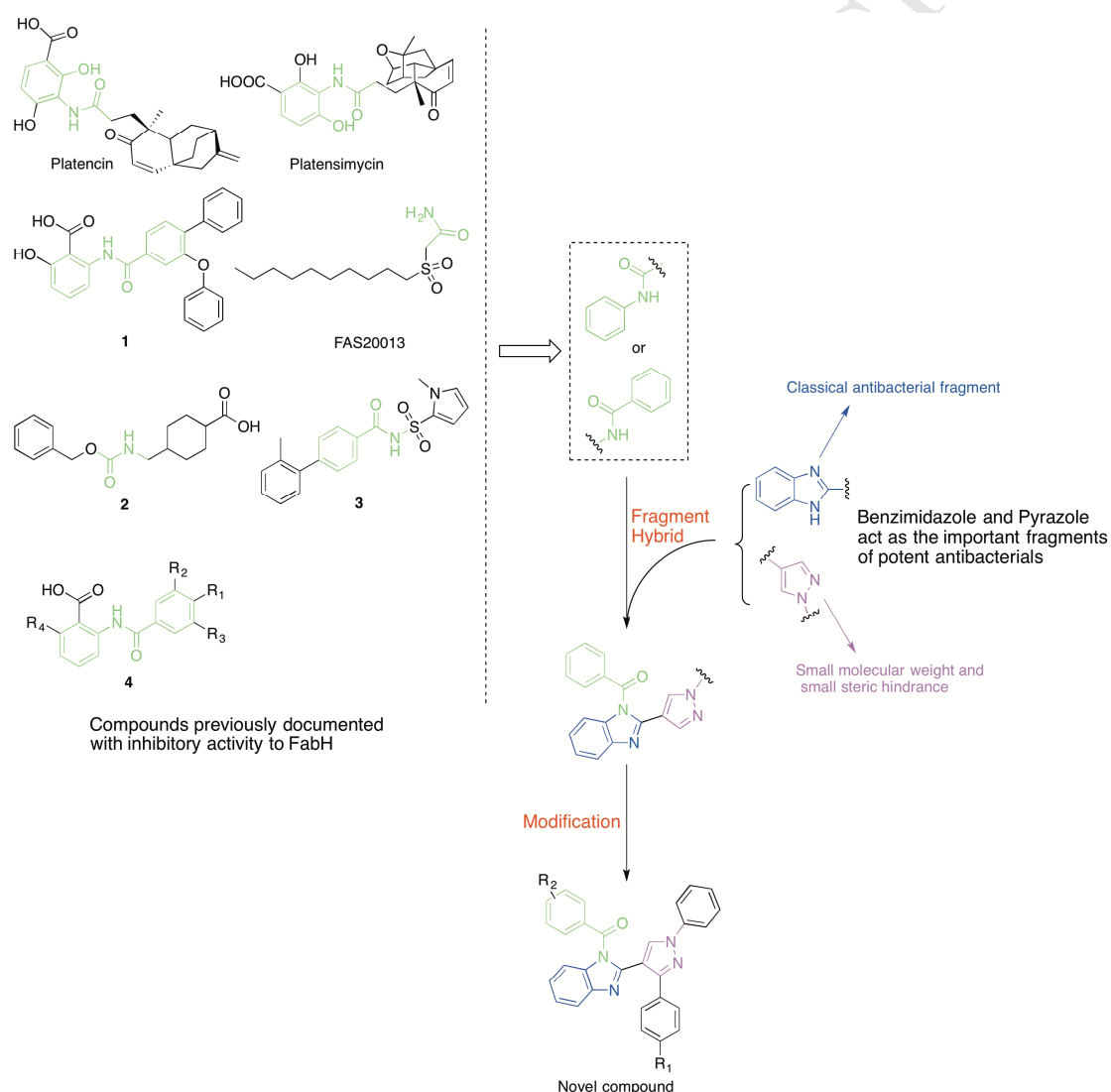


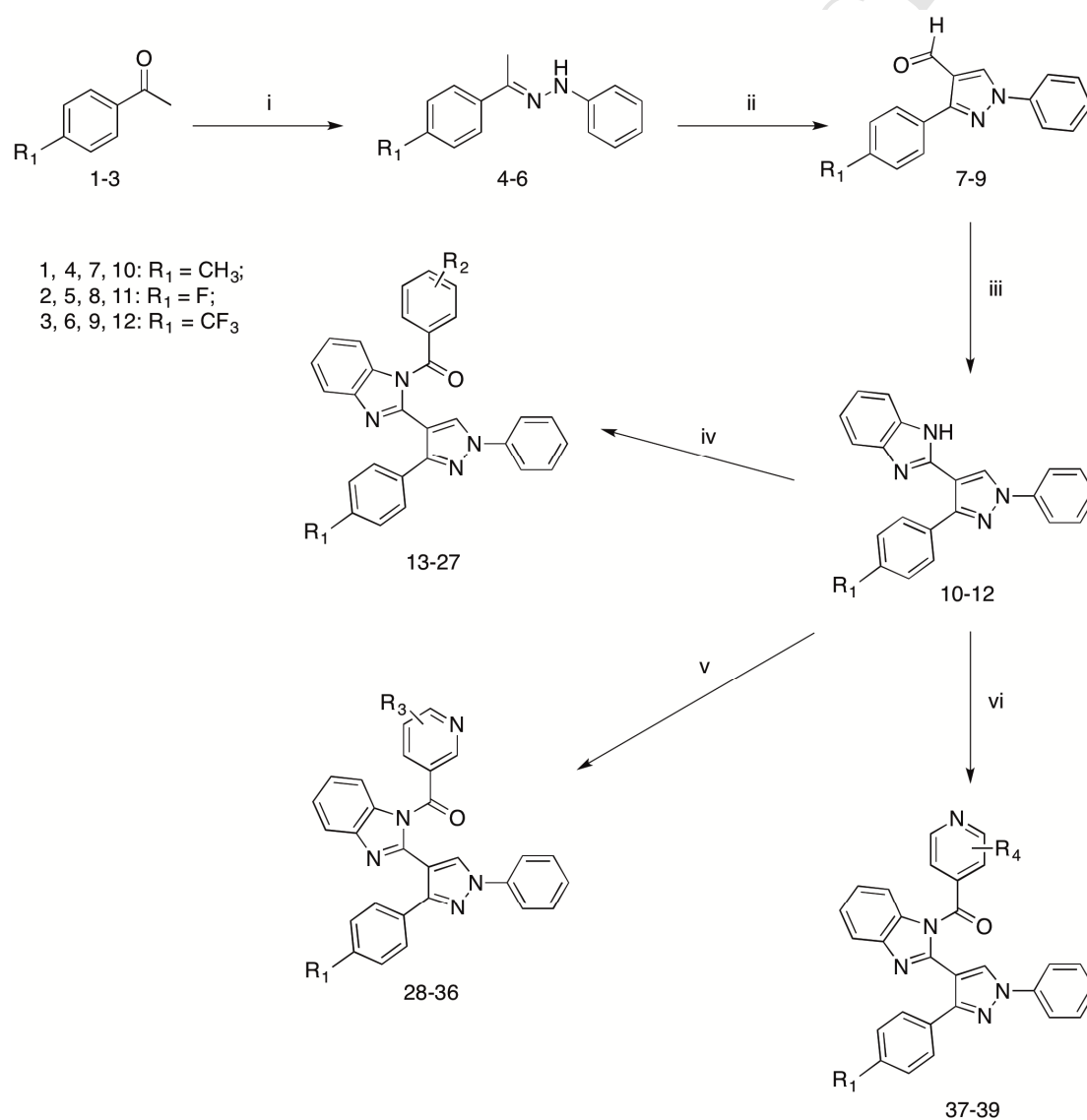
Fig. 2. Reported antibacterial agents targeting FabH and fragment hybrid of selected segments for the design of novel compounds binding to FabH.

2. Results and discussion:

2.1. Chemistry

The synthesis of compounds **13-39** followed the general pathway was outlined in Scheme 1. The target compounds were obtained in four steps as described in experimental section. All of the synthetic compounds are being reported for the first time (Table 1) and gave satisfactory analysis and spectroscopic data. ^1H NMR, ^{13}C NMR, melting test and mass spectroscopy, and analysis results were in full accordance with their depicted structures.

Scheme 1^a General synthesis of compounds **13-39**.



^a Reagents and conditions: (i) sodium acetate, phenylhydrazine hydrochloride, H₂O, rt, 3 h; (ii) POCl₃, DMF, 58 °C, 5 h, reflux; (iii) *o*-diaminobenzene, sodium metabisulfite, DMF, 110 °C, 4 h, reflux; (iv) benzoic acid, DMAP, EDC·HCl, DCM, rt, 4 h; (v) nicotinic acid, DMAP, EDC·HCl, DCM, rt, 4 h; (vi) isonicotinic acid, DMAP, EDC·HCl, DCM, rt, 4 h.

Table 1. Structures of compounds **13-39**

Compound	R ₁	R ₂	Compound	R ₁	R ₃	R ₄
13	CH ₃	H	28	CH ₃	H	-
14	CH ₃	2-CH ₃	29	CH ₃	5-CH ₃	-
15	CH ₃	3-CH ₃	30	CH ₃	6-CH ₃	-
16	CH ₃	4-CH ₃	31	F	H	-
17	CH ₃	4-Cl	32	F	5-CH ₃	-
18	F	H	33	F	6-CH ₃	-
19	F	2-CH ₃	34	CF ₃	H	-
20	F	3-CH ₃	35	CF ₃	5-CH ₃	-
21	F	4-CH ₃	36	CF ₃	6-CH ₃	-
22	F	4-Cl	37	CH ₃	-	H
23	CF ₃	H	38	F	-	H
24	CF ₃	2-CH ₃	39	CF ₃	-	H
25	CF ₃	3-CH ₃				
26	CF ₃	4-CH ₃				
27	CF ₃	4-Cl				

2.2. Crystal structure determination

The crystal structures of compound **17** were determined by X-ray diffraction analysis. The crystal data presented in Table 2 and Fig. 3 gave the perspective views of **17** with the atomic labeling system. The crystallographic data have been deposited at the Cambridge Crystallographic Data Centre (CCDC) and the deposition number of **17** is 1494813.

Table 2. Crystallographic and experimental Data for compound **17**

Compound	17
----------	-----------

Formula	C ₃₀ H ₂₁ ClN ₄ O	Z	4
Formula weight	488.98	D _c (g•cm ⁻³)	1.339
Crystal system	Monoclinic	μ(mm ⁻¹)	0.189
Space group	P-1	F(000)	1016
a (Å)	10.062(3)	θrang(°)	2.11- 28.76
b (Å)	10.864(3)	Reflns collected	10275
c (Å)	23.171(6)	Reflns unique	651
α(°)	89.852(7)	Goodness-of-fit on F ²	1.048
β(°)	89.696(7)	RI, wR ₂ [I>2σ(I)]	0.0777, 0.2074
γ(°)	73.268(7)	RI, wR ₂ [all data]	0.0989, 0.2275
V(Å ³)	2425.6(11)	Max, minΔρ(e Å ⁻³)	0.539, -0.538

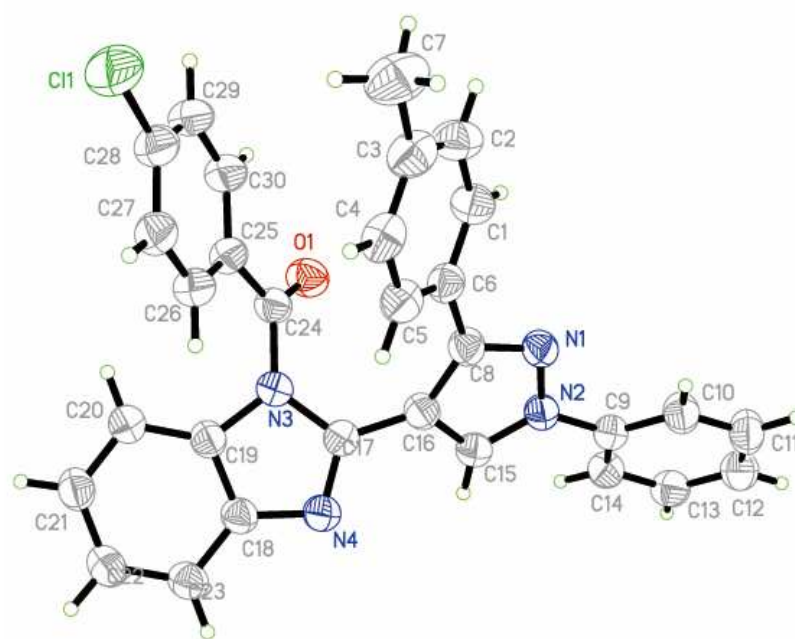


Fig. 3. ORTEP drawing of the crystal structure of **17**

2.3. Biological activity

2.3.1. Antibacterial activity

Two Gram-negative bacterial strains: *E. coli* and *P. aeruginosa* and two Gram-positive bacterial strains: *B. subtilis* and *S. aureus* were exploited in the antimicrobial assay. All the synthesized compounds **13-39** were evaluated for their antibacterial activity with TTC double dilution method, with DDCP and kanamycin B

as controls. The results were listed in Table 3, and as shown, the MIC (minimum inhibitory concentration) value indicated that these novel compounds showed better inhibitory activity against *B. subtilis* than other bacteria. Some of them possessed potent activity, for example, compounds **16**, **21**, **26**, **28**, **30**, **31**, **33**, **34**, **35** and **36** exerted the similar inhibitory activity with the controls. Notably, compound **31** exhibited the most potent activity and broad-spectrum antibacterial activity against all the four bacteria strains, with MIC of 0.98, 0.49, 0.98, 0.98 $\mu\text{g/mL}$, respectively for *E. coli*, *P. aeruginosa*, *B. subtilis* and *S. aureus*, which was better than the positive controls DDCP (3.9, 0.98, 3.9, 1.95 $\mu\text{g/mL}$) and kanamycin B (1.95, 3.9, 0.98, 0.98 $\mu\text{g/mL}$).

According to the data listed in Table 3, we could arrive at the conclusion that the activity of the tested compounds may be correlated to the variation and modification of the structure. Structure-activity relationship (SAR) analysis demonstrated that type and location of the substituent have important influences on the antibacterial activity.

We drew that nicotinic groups have better antibacterial effects than benzoic acid groups according to the activity data: **28-39** overall exhibited better antibacterial activities than **13-27**. At the position of R_1 of the benzene ring attached to the pyrazole, the order of activity of the group introduced is $4\text{-F} > 4\text{-CF}_3 > 4\text{-CH}_3$, indicating that introduction of a halogen group at R_1 enhances the antibacterial activity.

Among compounds **13-27**, different substituents were confirmed. With R_1 fixed, 4-CH_3 or 4-Cl was introduced at the R_2 position, and data showed that the activity sequence was $4\text{-CH}_3 > 4\text{-Cl}$. The results showed that the introduction of an electron-donating group at R_2 can enhance the antibacterial activity. In addition, substituents at different positions are evaluated as well. Also with R_1 fixed, 2-CH_3 / 3-CH_3 / 4-CH_3 is introduced at the R_2 position, and the order of activity from the antibacterial data is *para-* > *meta-* > *ortho-* ($5\text{d} > 5\text{j} > 5\text{m}$, $5\text{c} > 5\text{k} > 5\text{n}$, $5\text{f} > 5\text{l} > 5\text{o}$).

Furthermore, among compounds **28-39**, when the R_1 position was fixed and -H , 5-CH_3 , 6-CH_3 was introduced at the R_3 position, the activity sequence can be obtained from the antibacterial data $\text{-H} < 6\text{-CH}_3 < 5\text{-CH}_3$ (**35** < **36** < **34**, **32** < **33** < **31**), indicating that H at R_3 enhances antibacterial activity. Compounds **37**, **38**, **39** have lower antibacterial activity, demonstrating that isonicotinic acid groups can not enhance antibacterial activity.

Then, we drew two conclusions as follows: (1) F substituent in R₁ could enhance antibacterial activity. (2) Nicotinic acid group substitution linked to amide bonds could also increase the activity. (3) Electron-donating groups and *para*-substituent at R₂ can enhance the antibacterial activity.

Table 3. MIC of synthetic compounds against bacteria and IC₅₀ against FabH

Compounds	MIC ($\mu\text{g/mL}$)				<i>E. coli</i> FabH ^b IC ₅₀ \pm SD (μM)
	Gram-negative		Gram-positive		
	<i>E. coli</i>	<i>P. aeruginosa</i>	<i>B. subtilis</i>	<i>S. aureus</i>	
13	>62.5	62.5	31.25	>62.5	28.23 \pm 0.32
14	62.5	>62.5	62.5	>62.5	35.41 \pm 0.13
15	62.5	62.5	31.25	>62.5	33.17 \pm 0.13
16	3.9	31.25	0.98	>62.5	3.06 \pm 0.12
17	62.5	>62.5	62.5	>62.5	38.24 \pm 0.25
18	62.5	62.5	7.8	>62.5	22.08 \pm 0.21
19	>62.5	>62.5	62.5	>62.5	37.23 \pm 0.15
20	62.5	31.25	31.25	62.5	34.11 \pm 0.38
21	62.5	>62.5	0.98	>62.5	30.33 \pm 0.21
22	62.5	>62.5	62.5	>62.5	36.09 \pm 0.13
23	62.5	62.5	15.6	>62.5	25.65 \pm 0.24
24	>62.5	>62.5	62.5	>62.5	36.45 \pm 0.27
25	62.5	31.25	31.25	>62.5	34.86 \pm 0.29
26	62.5	>62.5	3.9	>62.5	31.82 \pm 0.36
27	62.5	31.25	62.5	>62.5	39.81 \pm 0.25
28	62.5	62.5	0.98	31.25	18.33 \pm 0.23
29	62.5	62.5	7.8	62.5	9.56 \pm 0.13
30	62.5	62.5	0.98	62.5	16.88 \pm 0.13
31	0.98	0.49	0.98	0.98	1.22 \pm 0.23
32	62.5	62.5	15.6	62.5	22.09 \pm 0.19
33	1.95	62.5	0.98	62.5	4.02 \pm 0.34
34	62.5	62.5	1.95	62.5	15.23 \pm 0.19
35	62.5	62.5	0.98	62.5	22.89 \pm 0.39
36	1.95	62.5	0.49	62.5	2.05 \pm 0.21
37	>62.5	62.5	31.25	62.5	33.88 \pm 0.13
38	>62.5	62.5	7.8	62.5	32.67 \pm 0.22

39	>62.5	62.5	31.25	62.5	30.28±0.24
DDCP	3.9	0.98	3.9	1.95	1.56±0.18
Kanamycin B	1.95	3.9	0.98	0.98	-

^{a,b} Values represent the average of three independent experiments run in triplicate.

2.3.2. *E. coli* FabH inhibitory activity of synthetic compounds

To generate data concerning the broad-spectrum potential of these novel compounds in Table 1, FabH enzymes inhibition activities were determined by MTT assay, and the IC₅₀ values were summarized in Table 3. As shown, to some extent the antibacterial potential is consistent with the enzyme inhibition of *E. coli* FabH, with a few exceptions. In detail, compounds with low antibacterial activity showed poor *E. coli* FabH enzyme inhibitory activity, with IC₅₀ >25 μM; compounds possessing potent activity against *E. coli* are generally endowed with significant potential against the enzyme *E. coli* FabH, with IC₅₀ of 1.22-22.89 μM.

The IC₅₀ values of compounds **28-39** are generally lower than 25 μM, while IC₅₀ of **13-27** is generally higher than 25 μM, which demonstrated that the introduction of nicotinic acid groups enhances the inhibitory activity of *E. coli* FabH enzyme. From the *E. coli* FabH enzyme inhibitory activity sequence **31** > **34** > **28** and **18** > **23** > **13**, it was concluded that the F substituent at R₁ (halogen group) enhances the *E. coli* FabH enzyme inhibitory activity. Besides, among compounds **28-39**, H at R₃ showed the most potent *E. coli* FabH enzyme inhibitory activity. In addition, among compounds **13-27**, electron donating group introduced at R₂ has the lowest IC₅₀ value and the highest enzyme inhibitory activity. Further, during all the compounds, **31** exhibited the most potent *E. coli* FabH enzyme inhibitory activity, with IC₅₀ of 22.89 μM, which was better than the positive control DDCP (IC₅₀=1.56 μM). Then, it is concluded that the antibacterial ability of the compounds is related to the inhibition of FabH enzyme, for the FabH inhibition having a positive correlation with the antibacterial activity.

2.3.3. Antibacterial experiment on wild type and FabH mutant *Xanthomonas Campestris*

To further explain that the antibacterial effect is achieved by inhibiting FabH, wild type strain *Xanthomonas oryzae* pv. *Oryza* KACC10331 and mutant strain *Xanthomonas oryzae* pv. *Oryza* KACC10331 Δ FabH were chosen for MIC experiments.

Table 4. MIC ($\mu\text{g/mL}$) of selected compounds against wild type and mutant *Xanthomonas Campestris* strains.

Compounds	<i>Xanthomonas oryzae pv.</i>	<i>Xanthomonas oryzae pv. Oryza</i>
	<i>Oryza</i> KACC10331	KACC10331 Δ FabH
30	15.63	>62.5
31	0.49	>62.5
33	15.63	>62.5
34	15.63	>62.5
35	7.82	>62.5

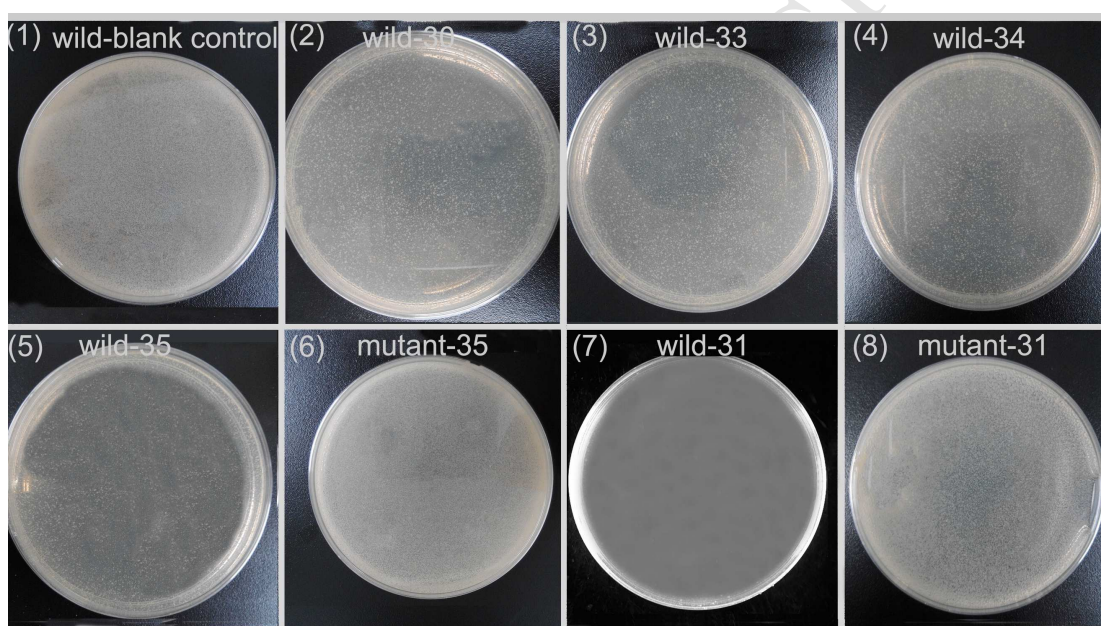


Fig. 4. **30**, **31**, **33**, **34** and **35** were assessed against two types of *Xanthomonas oryzae pv. Oryza* KACC10331 (wild type and mutant type). $5 \mu\text{g/mL}$ of each compound was added onto two types of strains. (1) wild type strain without compound treating; (2), (3), (4), (5), (7) **30**, **33**, **34**, **35** and **31** acted on wild type strain, respectively; (6), (8) mutant type of strain were treated with **35** and **31**, respectively.

Five of the most potent analogues, **30**, **31**, **33**, **34** and **35** were assessed against the two strains (Table 4 and Fig. 4). As Table 4 depicted, they all showed significant inhibition, especially **31** emerged as the most potent analogue with MIC of $0.49 \mu\text{g/mL}$, however, all the selected compounds exhibited no inhibition against FabH-deficient mutant strain. In addition, Fig. 4 exhibited the effect of $5 \mu\text{g/mL}$ of each compound on two types of *Xanthomonas oryzae pv. Oryza* KACC10331 (wild type and mutant type), and the results were in accordance with Table 4. Compound **31**

displayed the strongest inhibition against wild type bacterial, and no bacteria was seen in the medium plate treated with 5 $\mu\text{g}/\text{mL}$ of **31**, then effect of **35** followed after **31**. Also, almost no inhibition was found in the acting on **31** and **35** against mutant type bacterial. Consequently, this experiment firmly suggested the series of compounds arrived at antibacterial activity via inhibiting FabH.

2.3.4. Cytotoxicity and hemolytic activities

For the sake of seeking for potent antibiotics, testing safety of these compounds is significant. One of the main obstacles to the clinical use of compounds with effective antibacterial activities is their degree of injury to mammalian cell that leads to high hemolytic and cytotoxic activity dangerous to the host organism. Hemolytic activity is conventionally used as a measure of cytotoxicity and model for mammalian cells because red blood cells are, in general, extremely fragile. However, sometimes compounds which show low hemolytic activities have the severe cytotoxicity against mammalian cells. So the hemolysis and 293T cell (human kidney epithelial cell) cytotoxicity assays were both tested. Overall, as shown in Table 5, these compounds displayed low hemolytic activities. Besides, based on the data above, it showed that the compounds with potent antibacterial inhibitory activity were low toxic.

Table 5. Human kidney epithelial cell cytotoxicity (CC_{50} , μM) and hemolytic activities (LC_{30} , mg/mL) of tested compounds

Compounds	293T	Hemolysis	Compounds	293T	Hemolysis
	(^a CC_{50} , μM)	(^b LC_{30} (mg/mL))		(^a CC_{50} , μM)	(^b LC_{30} (mg/mL))
13	203.53 \pm 0.22	>10	27	180.91 \pm 0.23	>10
14	175.76 \pm 0.12	>10	28	189.36 \pm 0.26	>10
15	195.47 \pm 0.14	>10	29	155.45 \pm 0.25	>10
16	175.75 \pm 0.31	>10	30	145.42 \pm 0.16	>10
17	215.78 \pm 0.28	>10	31	215.54 \pm 0.23	>10
18	179.62 \pm 0.11	>10	32	119.44 \pm 0.25	>10
19	188.59 \pm 0.18	>10	33	136.51 \pm 0.14	>10
20	147.61 \pm 0.31	>10	34	158.22 \pm 0.15	>10
21	178.43 \pm 0.43	>10	35	123.46 \pm 0.14	>10
22	178.89 \pm 0.15	>10	36	153.23 \pm 0.26	>10
23	168.37 \pm 0.25	>10	37	150.59 \pm 0.24	>10

24	179.34±0.31	>10	38	134.56±0.35	>10
25	154.46±0.22	>10	39	153.64±0.16	>10
26	168.62±0.44	>10	DDCP	201.23±0.12	>10

^{a,b} Values are the average of three independent experiments run in triplicate.

2.4. ADMET model

For *in silico* study, the ADMET (Absorption, Distribution, Metabolism, Excretion, Toxicity) simulation [28-30] for **13-39** was initially depicted in Fig. 5 The parameters of AlogP (the partition coefficient of drug in octanol/aqueous solution calculated by ACD/PhysChem Suite Software) and PSA_{2D} (the fast calculated polar surface area from the 2D structure) were used to predict the Absorption (human intestinal absorption) and BBB (blood-brain barrier penetration) including 95% and 99% confidence ellipses as referenced [30]. All the compounds suggested good potential in druggability, which are potential for oral administration with low side effects.

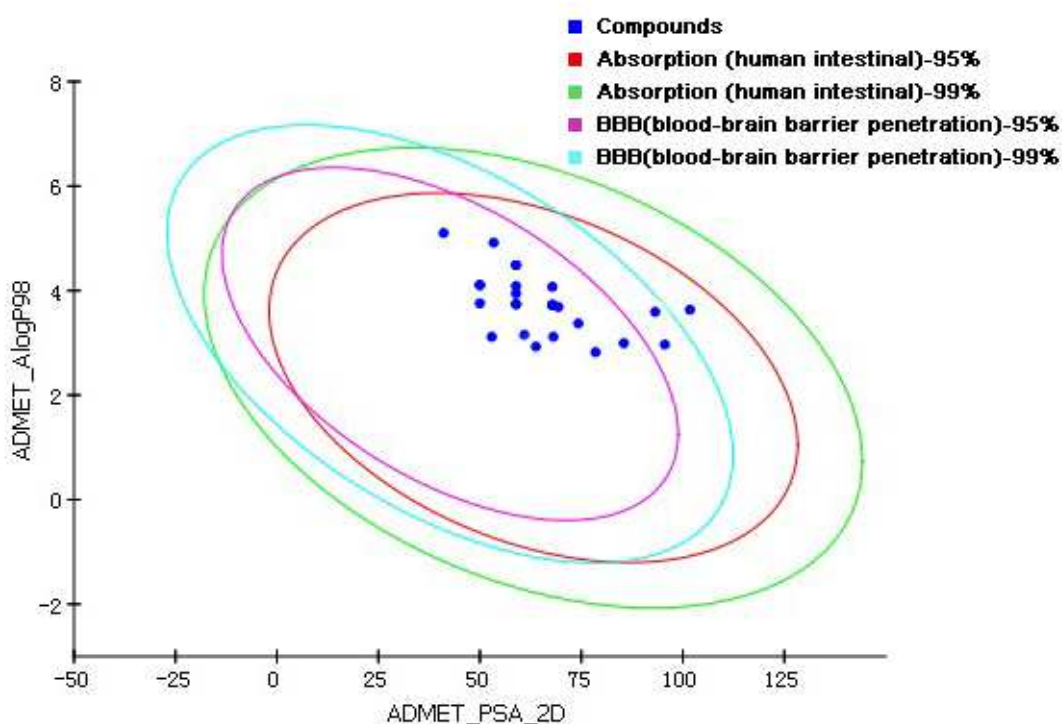


Fig. 5. ADMET properties predicted for compounds **13-29**. Compounds located inside the innermost oval are better for this parameter. Only **32**, **35** and **38** were outside the innermost oval. The percentages in the figure legend meant the 95% and 99% confidence ellipses.

2.5. Molecular docking

Docking is an effective and reliable approach to simulate the probable binding mode of ligands and proteins. To visualize the possible binding model of interactions between a protein (enzyme) and small molecules (ligands) were the molecular docking techniques used [31]. Molecular modelling in this study was conducted by using CDOCKER protocol in Discovery Studio 3.5 (Discovery Studio 3.5, Accelrys, Inc. San Diego, CA). All twenty-seven compounds were docked into the active site of the receptor FabH (PDB code: 1HNJ), and effective docking scores of all the compounds have been recorded. As depicted in Fig. 6, the CDOCKER Interaction Energy (interaction energy between the ligand and the receptor) was coincident with the *E.coli* FabH enzyme inhibitory activity trend for all compounds, and compound **31** showed the lowest energy value (-54.46 kcal/mol), which represented the most potent binding affinity. This result hinted the consistency of the SAR and molecular docking. Furthermore, the interacting model between protein receptor 1HNJ and the most potent compound **31** was investigated. 2D and 3D maps of them were depicted in Fig. 7, showing both the detailed surrounding situation and the laconic binding site. Seen in Fig. 7, **31** formed three hydrogen bonds with ARG36 (O \cdots H-N: 3.37 Å), ARG36 (O \cdots H-N: 3.04 Å) and ASN210 (O \cdots H-N: 3.22 Å), indicating benzimidazole amide was favorable for the activity increase. Amide- π interaction between pyrazole and GLY209 (distance: 4.91 Å), π - π interaction between benzene ring neighboring to pyrazole and PHE213 (distance: 5.11 Å) and π -cation interaction between the same benzene ring and ARG249 (distance: 4.12 Å) maintained the basic binding pattern of this series. Besides, the high affinity of compound **31** with 1HNJ may also be caused by some weak interactions, such as Van der Waals' force.

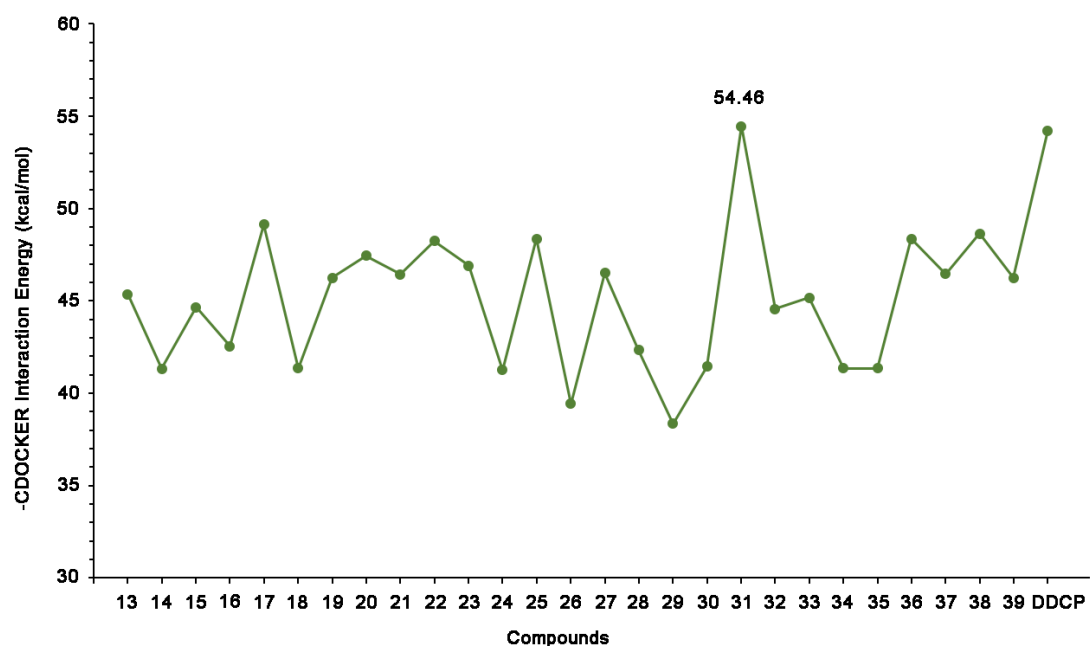


Fig. 6. The histogram about CDOCKER_INTERACTION_ENERGY (-kcal/mol) of compounds (13 - 39 and DDCP) for FabH, in the binding mode, compound 31 had a best estimated binding free energy of -54.46 kcal/mol.

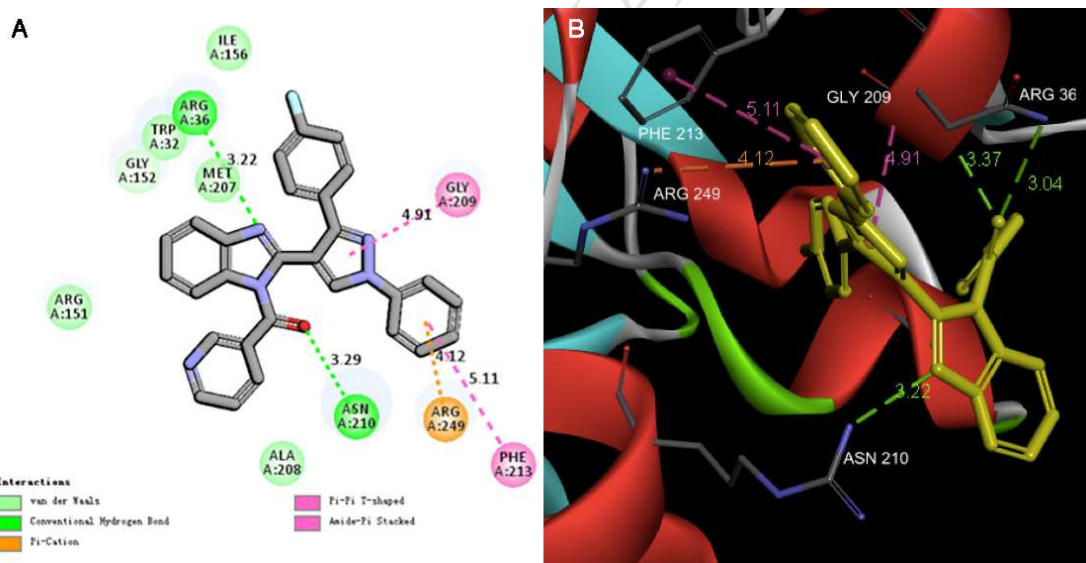


Fig. 7. Docking models of representative compound 31. (A) 2D molecular docking modeling of compound 31 and surrounding residues of *E. coli* FabH (PDB code: 1HNJ). (B) 3D molecular docking modeling of compound 31 with *E. coli* FabH.

2.6 Lipinski's rule-of-five

In addition, this class of compounds were evaluated compliance with Lipinski's rule-of-five (Molecular weight (MW) \leq 500D, Number of hydrogen bond donors (HBD) \leq 5, Number of hydrogen bond acceptors (HBA) \leq 10, $-2\leq$ calculated lipophilicity ($\log P$) \leq 5, Number of rotatable bonds (NRB) \leq 10) for the preliminary screening. The

indicator results were depicted in Table 6. According to this analysis, one can conclude that this series of compounds showed excellent pharmacokinetic properties, and could be used to improve novel attractive compounds.

Table 6 Calculated percentiles of main descriptors for these compounds.

Descriptor	MW	NRB	log P	HBA	HBD
Data	454.53-542.95	6-10	4.2-7.8	1-5	0-6

3. Conclusion

Overall, we have designed and synthesized twenty-seven new FabH inhibitors. They exhibited excellent activity against both Gram-positive and Gram-negative bacteria, as well as FabH inhibitory activity. The cytotoxicity test employing human kidney epithelial cell 293T and hemolysis test indicated high safety. Of all these compounds, compound **31** showed the most potent inhibition activity against four bacteria strains (with MIC of 0.98, 0.49, 0.98, 0.98 $\mu\text{g/mL}$, respectively against *E. coli*, *P. aeruginosa*, *B. subtilis* and *S. aureus*) and FabH (with IC_{50} of 1.22 μM). FabH mutant *Xanthomonas Campestris* experiment validated that compounds binding site outcomes FabH. Additionally, *in silico* ADMET evaluation also pointed out that these compounds are potential for oral administration with low side effects. Furthermore, the probable binding mode proposed by the docking simulation may be a good explanation of the impressive performance of **31**, in which **31** binds well with FabH via three hydrogen bonds, an amide- π interaction, a π - π interaction and a π -cation interaction.

4. Experimental section

4.1. Materials and measurements

All chemicals and reagents used in current study were analytical grade. Thin layer chromatography (TLC), proton nuclear magnetic resonance (^1H NMR) and elemental microanalyses (CHN) were usually used. Analytical thin-layer chromatography (TLC) was performed on the glass-backed silica gel sheets (silica gel 60 Å GF254). All compounds were detected using UV light (254 nm or 365 nm). Separation of the compounds by column chromatography was carried out with silica

gel 60 (200 – 300 mesh ASTM, E. Merck). The quantity of silica gel used was 50-100 times the weight charged on the column. Melting points were determined on a XT4 MP apparatus (Taikē Corp., Beijing, China). ¹H NMR spectra were measured on a Bruker DPX 400 spectrometer at 25 °C and referenced to Me₄Si. Chemical shifts are reported in ppm (δ) using the residual solvent line as internal standard. Splitting patterns are designed as s, singlet; d, doublet; t, triplet; m, multiplet. ESI-MS spectra were recorded on a Mariner System 5304 Mass spectrometer. Elemental analyses were performed on a CHN-O-Rapid instrument and were within \pm 0.4% of the theoretical values.

4.2. General procedure for preparation of 1-phenyl-2-(1-(*p*-tolyl)ethylidene)hydrazine (4) [32, 33]

To prepared compound **4**, *p*-methylacetophenone (compound **1**, 6.71 g, 50 mmol) was reacted with phenylhydrazine hydrochloride (8.68 g, 60 mmol) at the presence of sodium acetate (10.21 g, 75 mmol) in water (120 mL). After stirring at room temperature for 3.5 h, a large amount of yellow solid emerged and was filtered to give compound **4** (yields 95 %). The corresponding substituted 1-phenyl-2-(1-phenylethylidene) hydrazines followed this way to prepare pure compounds **5** and **6** with yields of 91% and 96%.

4.3. General procedure for preparation of 1-phenyl-3-(*p*-tolyl)-1*H*-pyrazole-4-carbaldehyde (7) [32, 33]

Compound **4** (8.97 g, 40 mmol) was treated with Vilsmeier-Haack reagent (DMF-POCl₃, 30 mL DMF and 10 mL POCl₃). After stirring at 55 °C for 6 h, the mixture was poured into ice-cold water, with a saturated solution of sodium hydroxide being added to neutralize the mixture. Then a large amount of solid emerged, which was filtered, washed with water, and dried to give compound **7** (yields 91 %). The corresponding substituted 1,3-diphenyl-1*H*-pyrazole-4-carbaldehydes were synthesized following this way to receive pure compounds **8** and **9** with a yield of 88% and 93%.

4.4. General procedure for preparation of 2-(1-phenyl-3-(*p*-tolyl)-1*H*-pyrazol-4-yl)-1*H*-benzo[d]imidazole (10) [34]

O-phenylenediamine (3.24 g, 30 mmol) was coupled with compound **7** (10.51 g, 30 mmol) in DMF (70 mL) at the presence of sodium pyrosulfite (11.41 g, 60 mmol). The heterogeneous mixture was stirred at 110 °C for 4 h, then cooled and poured onto

a lot of ice. A large amount of solid would emerge, and was filtered to give 2-(1-phenyl-3-(*p*-tolyl)-1*H*-pyrazol-4-yl)-1*H*-benzo[*d*]imidazole (**10**), a yellow powder, yielding 83%. The corresponding substituted 2-(1,3-diphenyl-1*H*-pyrazol-4-yl)-1*H*-benzo[*d*]imidazoles were synthesized following this way, and we got pure compounds **11** and **12** with a yield of 82% and 85%.

4.5. General synthesis method of 2-(1,3-diphenyl-1*H*-pyrazol-4-yl)-1*H*-benzo[*d*]imidazol-1-yl)(phenyl)methanone (**13**)

To obtain compound **13**, the intermediate product **10** (0.35 g, 1mmol) coupled with benzoic acid (0.18 g, 1.5 mmol) in 30 mL dichloromethane at room temperature for 4.5 h, with the help of triethylamine (2 - 3 drops), EDC·HCl (0.25 g, 1.3mmol) and DMAP (0.16 g, 1.3mmol). The reaction mixture was then extracted with dichloromethane (15 mL × 3) and distilled water (15 mL). After the solvent was evaporated under reduced pressure, products were purified by column chromatography on silica gel (200 - 300 mesh) using ethyl acetate / petroleum ether (v/v = 1:6) as eluent to yield pure compound **13** (yields 68 %). The corresponding substituted

2-(1,3-diphenyl-1*H*-pyrazol-4-yl)-1*H*-benzo[*d*]imidazol-1-yl)(phenyl)methanone compounds,

2-(1,3-diphenyl-1*H*-pyrazol-4-yl)-1*H*-benzo[*d*]imidazol-1-yl)(pyridin-3-yl)methanone compounds and

2-(1,3-diphenyl-1*H*-pyrazol-4-yl)-1*H*-benzo[*d*]imidazol-1-yl)(pyridin-4-yl)methanone compounds were prepared following this way, with yields of 56 - 82% for pure compounds **14** – **39**.

4.5.1. phenyl(2-(1-phenyl-3-(*p*-tolyl)-1*H*-pyrazol-4-yl)-1*H*-benzo[*d*]imidazol-1-yl)methanone (**13**)

White powder, yield: 87%. M. p: 146 - 147 °C, ¹H NMR (DMSO-*d*₆, 400 MHz) δ: 2.27 (s, 3H); 7.04 (d, *J* = 8, 2H); 7.25 - 7.31 (m, 4H); 7.36 - 7.40 (m, 4H); 7.47 - 7.50 (m, 3H); 7.52 - 7.55 (m, 2H); 7.79 (d, *J* = 5.2, 2H); 7.86 (d, *J* = 5.2, 1H); 8.84 (s, 1H). ESI-MS: 454.53 (C₃₀H₂₂N₄O, [M+H]⁺).

4.5.2. 2-(1-phenyl-3-(*p*-tolyl)-1*H*-pyrazol-4-yl)-1*H*-benzo[*d*]imidazol-1-yl)(*o*-tolyl)methanone (**14**)

White powder, yield: 69%. M. p: 165 - 167 °C, ¹H NMR (DMSO-*d*₆, 400 MHz) δ: 2.34 (s, 3H); 2.48 (s, 3H); 7.05 (s, 2H); 7.21 - 7.25 (m, 3H); 7.28 (s, 2H); 7.37 - 7.42 (m, 3H); 7.52 - 7.57 (m, 4H); 7.68 (s, 2H); 7.80 (s, 1H); 8.44 (s, 1H). ESI-MS: 468.56 (C₃₁H₂₄N₄O, [M+H]⁺).

4.5.3. (2-(1-phenyl-3-(*p*-tolyl)-1H-pyrazol-4-yl)-1H-benzo[d]imidazol-1-yl)

(*m*-tolyl)methanone (15)

Yellow powder, yield: 87%. M. p: 183 - 184 °C, ¹H NMR (DMSO-*d*₆, 400 MHz) δ: 2.34 (s, 3H); 2.37 (s, 3H); 6.66 - 6.68 (m, 1H); 6.76 (d, *J* = 5.2, 1H); 7.07 - 7.09 (m, 1H); 7.21 (d, *J* = 4.8, 1H); 7.26 (d, *J* = 5.2, 2H); 7.29 - 7.31 (m, 1H); 7.38 (d, *J* = 3.2, 2H); 7.49 - 7.51 (m, 2H); 7.70 (d, *J* = 5.6, 2H); 7.76 (d, *J* = 12, 2H); 7.82 (d, *J* = 5.2, 2H); 8.51 (s, 1H). ESI-MS: 468.56 (C₃₁H₂₄N₄O, M+H)⁺.

4.5.4. (2-(1-phenyl-3-(*p*-tolyl)-1H-pyrazol-4-yl)-1H-benzo[d]imidazol-1-yl)

(*p*-tolyl)methanone (16)

White powder, yield: 60%. M. p: 159 - 161 °C, ¹H NMR (DMSO-*d*₆, 400 MHz) δ: 2.24 (d, *J* = 2.8, 6H); 7.11 (d, *J* = 5.2, 4H); 7.28 - 7.31 (m, 4H); 7.34 - 7.53 (m, 4H); 7.54 - 7.55 (m, 2H); 7.80 - 7.85 (m, 3H); 8.85 (s, 1H). ESI-MS: 468.56 (C₃₁H₂₄N₄O, [M+H]⁺). Anal.

4.5.5. (4-chlorophenyl)(2-(1-phenyl-3-(*p*-tolyl)-1H-pyrazol-4-yl)-1H-benzo[d]

imidazol-1-yl)methanone (17)

Yellow powder, yield: 65%. M. p: 181 - 182 °C, ¹H NMR (DMSO-*d*₆, 400 MHz) δ: 2.21 (s, 3H); 7.08 (d, *J* = 5.6, 2H); 7.12 - 7.14 (m, 2H); 7.32 (s, 3H); 7.36 - 7.39 (m, 2H); 7.41 - 7.46 (m, 2H); 7.51 - 7.66 (m, 3H); 7.75 (d, *J* = 5.2, 2H); 7.83 (d, *J* = 5.6, 1H); 8.74 (s, 1H). ESI-MS: 488.98 (C₃₀H₂₁ClN₄O, [M+H]⁺).

4.5.6. (2-(3-(4-fluorophenyl)-1-phenyl-1H-pyrazol-4-yl)-1H-benzo[d]imidazol-1-

yl)(phenyl)methanone (18)

White powder, yield: 66%. M. p: 172 - 174 °C, ¹H NMR (DMSO-*d*₆, 400 MHz) δ: 7.18 - 7.21 (m, 2H); 7.29 - 7.31 (m, 2H); 7.37 - 7.39 (m, 2H); 7.42 - 7.55 (m, 8H); 7.80 (d, *J* = 5.2, 2H); 7.86 (d, *J* = 5.2, 2H); 8.87 (s, 1H). ESI-MS: 458.50 (C₂₉H₁₉FN₄O, [M+H]⁺). Anal.

4.5.7. (2-(3-(4-fluorophenyl)-1-phenyl-1H-pyrazol-4-yl)-1H-benzo[d]imidazol-1-

yl)(*o*-tolyl)methanone (19)

Yellow powder, yield: 66%. M. p: 156 - 157 °C, ¹H NMR (DMSO-*d*₆, 400 MHz) δ: 2.02 (s, 3H); 7.09 - 7.12 (m, 2H); 7.22 - 7.28 (m, 3H); 7.37 - 7.40 (m, 2H); 7.43 - 7.47

(m, 2H); 7.54 - 7.59 (m, 4H); 7.65 (d, $J = 5.2$, 1H); 7.77 (d, $J = 5.2$, 2H); 7.88 (d, $J = 4.8$, 1H); 8.81 (s, 1H). ESI-MS: 472.52 ($C_{30}H_{21}FN_4O$, $M+H$)⁺.

4.5.8. (2-(3-(4-fluorophenyl)-1-phenyl-1H-pyrazol-4-yl)-1H-benzod[jimidazol-1-yl](m-tolyl)methanone (20)

Yellow powder, yield: 67%. M. p: 214 - 215 °C, ¹H NMR (DMSO-*d*₆, 400 MHz) δ : 2.09 (s, 3H); 7.16 - 7.24 (m, 5H); 7.28 (d, $J = 4.8$, 1H); 7.37 - 7.40 (m, 2H); 7.43 - 7.44 (m, 1H); 7.47 - 7.50 (m, 2H); 7.53 - 7.55 (m, 3H); 7.78 (d, $J = 5.2$, 2H); 7.86 (d, $J = 5.2$, 1H); 8.85 (s, 1H). ESI-MS: 472.52 ($C_{30}H_{21}FN_4O$, $M+H$)⁺.

4.5.9. (2-(3-(4-fluorophenyl)-1-phenyl-1H-pyrazol-4-yl)-1H-benzod[jimidazol-1-yl](p-tolyl)methanone (21)

White powder, yield: 70%. M. p: 187 - 189 °C, ¹H NMR (DMSO-*d*₆, 400 MHz) δ : 2.25 (s, 3H); 7.13 - 7.19 (m, 4H); 7.34 - 7.43 (m, 6H); 7.47 - 7.50 (m, 2H); 7.53 - 7.56 (m, 2H); 7.81 - 7.86 (m, 3H); 8.87 (s, 1H). ESI-MS: 472.52 ($C_{30}H_{21}FN_4O$, $M+H$)⁺.

4.5.10. (4-chlorophenyl)(2-(3-(4-fluorophenyl)-1-phenyl-1H-pyrazol-4-yl)-1H-benzod[jimidazol-1-yl)methanone (22)

Yellow powder, yield: 67%. M. p: 177 - 178 °C, ¹H NMR (DMSO-*d*₆, 400 MHz) δ : 7.17 - 7.20 (m, 2H); 7.36 - 7.41 (m, 4H); 7.46 - 7.50 (m, 5H); 7.52 - 7.57 (m, 3H); 7.80 - 7.82 (m, 3H); 7.86 (d, $J = 5.2$, 1H). ESI-MS: 492.94 ($C_{29}H_{18}ClFN_4O$, $M+H$)⁺.

4.5.11. phenyl(2-(1-phenyl-3-(4-(trifluoromethyl)phenyl)-1H-pyrazol-4-yl)-1H-benzod[jimidazol-1-yl)methanone (23)

Yellow powder, yield: 66%. M. p: 192 - 194 °C, ¹H NMR (DMSO-*d*₆, 400 MHz) δ : 7.29 - 7.32 (m, 2H); 7.36 - 7.45 (m, 4H); 7.49 - 7.52 (m, 3H); 7.54 - 7.57 (m, 2H); 7.71 - 7.75 (m, 4H); 7.82 - 7.87 (m, 3H); 8.94 (s, 1H). ESI-MS: 508.50 ($C_{30}H_{19}F_3N_4O$, $[M+H]$)⁺.

4.5.12. (2-(1-phenyl-3-(4-(trifluoromethyl)phenyl)-1H-pyrazol-4-yl)-1H-benzod[jimidazol-1-yl](o-tolyl)methanone (24)

Yellow powder, yield: 56%. M. p: 171 - 172 °C, ¹H NMR (DMSO-*d*₆, 400 MHz) δ : 2.04 (s, 3H); 6.92 - 6.95 (m, 1H); 7.11 - 7.15 (m, 2H); 7.26 - 7.29 (m, 1H); 7.40 - 7.49 (m, 3H); 7.56 - 7.61 (m, 3H); 7.78 - 7.81 (m, 6H); 7.88 (d, $J = 5.2$, 1H); 8.88 (s, 1H). ESI-MS: 522.53 ($C_{31}H_{21}F_3N_4O$, $M+H$)⁺.

4.5.13. (2-(1-phenyl-3-(4-(trifluoromethyl)phenyl)-1H-pyrazol-4-yl)-1H-benzod[jimidazol-1-yl](m-tolyl)methanone (25)

White powder, yield: 66%. M. p: 199 - 201 °C, ¹H NMR (DMSO-*d*₆, 400 MHz) δ: 2.08 (s, 3H); 7.16 - 7.19 (m, 1H); 7.25 - 7.30 (m, 3H); 7.38 - 7.46 (m, 3H); 7.51 - 7.58 (m, 3H); 7.74 (d, *J* = 1.6, 4H); 7.82 - 7.83 (m, 2H); 7.87 (d, *J* = 5.2, 1H); 8.94 (s, 1H). ESI-MS: 522.53 (C₃₁H₂₁F₃N₄O, M+H)⁺.

4.5.14. (2-(1-phenyl-3-(4-(trifluoromethyl)phenyl)-1H-pyrazol-4-yl)-1H-benzo[d]imidazol-1-yl)(*p*-tolyl)methanone (26)

Yellow powder, yield: 76%. M. p: 188 - 189 °C, ¹H NMR (DMSO-*d*₆, 400 MHz) δ: 2.25 (s, 3H); 7.14 (d, *J* = 5.2, 2H); 7.30 - 7.36 (m, 2H); 7.39 - 7.43 (m, 4H); 7.55 - 7.58 (m, 2H); 7.69 (d, *J* = 1.6, 4H); 7.86 (d, *J* = 5.6, 3H); 8.96 (s, 1H). ESI-MS: 522.53 (C₃₁H₂₁F₃N₄O, M+H)⁺.

4.5.15. (4-chlorophenyl)(2-(1-phenyl-3-(4-(trifluoromethyl)phenyl)-1H-pyrazol-4-yl)-1H-benzo[d]imidazol-1-yl)methanone (27)

White powder, yield: 68%. M. p: 211 - 212 °C, ¹H NMR (DMSO-*d*₆, 400 MHz) δ: 7.38 - 7.46 (m, 6H); 7.51 - 7.53 (m, 2H); 7.56 - 7.58 (m, 2H); 7.68 - 7.72 (m, 4H); 7.84 - 7.87 (m, 3H); 8.96 (d, *J* = 7.6, 1H). ESI-MS: 542.95 (C₃₀H₁₈ClF₃N₄O, M+H)⁺.

4.5.16. (2-(1-phenyl-3-(*p*-tolyl)-1H-pyrazol-4-yl)-1H-benzo[d]imidazol-1-yl)(pyridin-3-yl)methanone (28)

Yellow powder, yield: 60%. M. p: 191 - 192 °C, ¹H NMR (DMSO-*d*₆, 400 MHz) δ: 2.28 (s, 3H); 7.15 (d, *J* = 5.2, 2H); 7.24 - 7.27 (m, 3H); 7.37 - 7.39 (m, 1H); 7.41 - 7.48 (m, 2H); 7.53 - 7.55 (m, 2H); 7.70 - 7.75 (m, 2H); 7.78 (d, *J* = 5.2, 2H); 7.88 (d, *J* = 5.2, 1H); 8.49 (s, 1H); 8.57 (d, *J* = 3.2, 1H); 8.87 (s, 1H). ESI-MS: 455.52 (C₂₉H₂₁N₅O, [M+H]⁺).

4.5.17. (5-methylpyridin-3-yl)(2-(1-phenyl-3-(4-(trifluoromethyl)phenyl)-1H-pyrazol-4-yl)-1H-benzo[d]imidazol-1-yl)methanone (29)

White powder, yield: 61%. M. p: 173 - 174 °C, ¹H NMR (DMSO-*d*₆, 400 MHz) δ: 2.29 (s, 3H); 7.15 - 7.16 (m, 2H); 7.22 - 7.24 (m, 2H); 7.37 - 7.40 (m, 1H); 7.43 - 7.47 (m, 2H); 7.48 - 7.50 (m, 1H); 7.53 - 7.56 (m, 2H); 7.75 - 7.79 (m, 3H); 7.87 - 7.88 (m, 1H); 8.26 (d, *J* = 1.2, 1H); 8.39 (d, *J* = 0.8, 1H); 8.87 (s, 1H). ¹³C NMR (DMSO-*d*₆, 100 MHz) δ: 17.72, 21.28, 112.35, 114.69, 119.10, 120.26, 125.34, 125.59, 127.49, 127.62, 128.51, 128.54, 129.03, 129.31, 129.72, 130.12, 130.22, 132.08, 132.47, 134.23, 137.80, 138.53, 139.25, 143.08, 146.58, 147.73, 150.71, 153.71, 167.21. ESI-MS: 523.52 (C₃₀H₂₀F₃N₅O, [M+H]⁺).

4.5.18. (6-methylpyridin-3-yl)(2-(1-phenyl-3-(*p*-tolyl)-1H-pyrazol-4-yl)-1H-benzo

[d]imidazol-1-yl)methanone (30)

Yellow powder, yield: 71%. M. p: 189 - 191 °C, ¹H NMR (DMSO-*d*₆, 400 MHz) δ: 2.25 (s, 3H); 2.36 (s, 3H); 7.11 - 7.14 (m, 3H); 7.22 (d, *J* = 5.2, 2H); 7.37 - 7.41 (m, 2H); 7.44 - 7.46 (m, 1H); 7.53 - 7.56 (m, 2H); 7.60 - 7.62 (m, 2H); 7.79 (d, *J* = 5.2, 2H); 7.86 (d, *J* = 5.2, 1H); 8.38 (d, *J* = 1.6, 1H); 8.85 (s, 1H). ¹³C NMR (DMSO-*d*₆, 100 MHz) δ: 31.21, 33.43, 112.31, 114.27, 119.32, 120.41, 122.52, 125.21, 125.37, 127.42, 127.71, 129.13, 129.37, 129.72, 132.06, 134.28, 137.90, 138.12, 139.39, 143.41, 146.85, 150.22, 151.15. ESI-MS: 469.55 (C₃₀H₂₃N₅O, [M+H]⁺).

4.5.19. (2-(3-(4-fluorophenyl)-1-phenyl-1H-pyrazol-4-yl)-1H-benzo[d]imidazol-1-yl)(pyridin-3-yl)methanone (31)

Yellow powder, yield: 72%. M. p: 169 - 170 °C, ¹H NMR (DMSO-*d*₆, 400 MHz) δ: 7.20 - 7.22 (m, 2H); 7.28 - 7.30 (m, 1H); 7.38 - 7.40 (m, 1H); 7.43 - 7.49 (m, 4H); 7.53 - 7.56 (m, 2H); 7.72 (d, *J* = 5.2, 1H); 7.78 (d, *J* = 5.6, 2H); 7.82 (d, *J* = 5.2, 1H); 7.88 (d, *J* = 5.2, 1H); 8.56 - 8.58 (m, 1H); 8.58 - 8.59 (m, 1H); 8.88 (s, 1H). ESI-MS: 459.48 (C₂₈H₁₈FN₅O, [M+H]⁺).

4.5.20. (2-(3-(4-fluorophenyl)-1-phenyl-1H-pyrazol-4-yl)-1H-benzo[d]imidazol-1-yl)(5-methylpyridin-3-yl)methanone (32)

White powder, yield: 70%. M. p: 157 - 158 °C, ¹H NMR (DMSO-*d*₆, 400 MHz) δ: 2.05 (s, 3H); 7.20 - 7.23 (m, 2H); 7.38 - 7.41 (m, 1H); 7.43 - 7.49 (m, 4H); 7.54 - 7.57 (m, 3H); 7.76 - 7.79 (m, 3H); 7.88 (d, *J* = 5.2, 1H); 8.33 - 8.40 (m, 2H); 8.89 (s, 1H). ESI-MS: 473.51 (C₂₉H₂₀FN₅O, [M+H]⁺).

4.5.21. (2-(3-(4-fluorophenyl)-1-phenyl-1H-pyrazol-4-yl)-1H-benzo[d]imidazol-1-yl)(6-methylpyridin-3-yl)methanone (33)

Yellow powder, yield: 74%. M. p: 149 - 150 °C, ¹H NMR (DMSO-*d*₆, 400 MHz) δ: 2.37 (s, 3H); 7.15 - 7.20 (m, 3H); 7.38 - 7.43 (m, 2H); 7.44 - 7.47 (m, 3H); 7.54 - 7.56 (m, 2H); 7.62 (d, *J* = 5.2, 1H); 7.68 - 7.70 (m, 1H); 7.79 (d, *J* = 5.2, 2H); 7.87 (d, *J* = 5.2, 1H); 8.45 (s, 1H); 8.87 (s, 1H). ESI-MS: 473.51 (C₂₉H₂₀FN₅O, [M+H]⁺).

4.5.22. (trifluoromethyl)phenyl)-1H-pyrazol-4-yl)-1H-benzo[d]imidazol-1-yl)(pyridin-3-yl)methanone (34)

White powder, yield: 56%. M. p: 182 - 184 °C, ¹H NMR (DMSO-*d*₆, 400 MHz) δ: 7.31 (s, 1H); 7.41 - 7.48 (m, 3H); 7.55 (d, *J* = 6.8; 2H); 7.67 - 7.88 (m, 9H); 8.61 (d, *J* = 8, 2H); 8.95 (s, 1H). ESI-MS: 509.49 (C₂₉H₁₈F₃N₅O, [M+H]⁺).

4.5.23. (5-methylpyridin-3-yl)(2-(1-phenyl-3-(4-(trifluoromethyl)phenyl)-1H-

pyrazol-4-yl)-1H-benzo[d]imidazol-1-yl)methanone (35)

Yellow powder, yield: 65%. M. p: 193 - 195 °C, ¹H NMR (DMSO-*d*₆, 400 MHz) δ: 2.05 (s, 3H); 7.42 - 7.48 (m, 3H); 7.55 - 7.59 (m, 2H); 7.64 (s, 1H); 7.74 (s, 5H) ; 7.81 (d, *J* = 8, 2H); 7.88 - 7.90 (m, 1H); 8.38 - 8.42 (m, 2H); 8.95 (s, 1H). ESI-MS: 523.52 (C₃₀H₂₀F₃N₅O, [M+H]⁺).

4.5.24. (6-methylpyridin-3-yl)(2-(1-phenyl-3-(4-(trifluoromethyl)phenyl)-1H-pyrazol-4-yl)-1H-benzo[d]imidazol-1-yl)methanone (36)

Yellow powder, yield: 75%. M. p: 188 - 190 °C, ¹H NMR (DMSO-*d*₆, 400 MHz) δ: 2.38 (s, 3H); 7.17 (d, *J* = 8, 1H); 7.40 - 7.46 (m, 3H); 7.54 - 7.59 (m, 3H); 7.69 (s, 4H); 7.72 - 7.75 (m, 1H); 7.82 - 7.88 (m, 3H); 8.51 (s, 1H); 8.96 (s, 1H). ESI-MS: 523.52 (C₃₀H₂₀F₃N₅O, [M+H]⁺).

4.5.25. (2-(3-(4-fluorophenyl)-1-phenyl-1H-pyrazol-4-yl)-1H-benzo[d]imidazole-1-yl)(pyridin-4-yl)methanone (37)

White powder, yield: 76%. M. p: 221 - 222 °C, ¹H NMR (DMSO-*d*₆, 400 MHz) δ: 7.21 - 7.31(m, 4H); 7.42 - 7.57 (m, 5H); 7.68 (s, 2H); 7.86 - 7.92 (m, 4H); 8.44 (s, 1H); 8.87 (s, 2H). ESI-MS: 459.48 (C₂₈H₁₈FN₅O, [M+H]⁺).

4.5.26. (2-(1-phenyl-3-(4-(trifluoromethyl)phenyl)-1H-pyrazol-4-yl)-1H-benzo[d]imidazol-1-yl)(pyridin-4-yl)methanone (38)

Yellow powder, yield: 65%. M. p: 149 - 150 °C, ¹H NMR (DMSO-*d*₆, 400 MHz) δ: 7.20 - 7.23 (m, 3H); 7.43 - 7.45 (m, 1H); 7.53 (d, *J* = 4.8, 1H); 7.60 - 7.65 (m, 4H); 7.83 (d, *J* = 5.6, 3H); 7.98 - 8.00 (m, 2H); 8.19 (d, *J* = 5.6, 2H); 9.16 (s, 1H); 12.62 (s, 1H). ESI-MS: 509.49 (C₂₉H₁₈F₃N₅O, [M+H]⁺).

4.5.27. (2-(1-phenyl-3-(*p*-tolyl)-1H-pyrazol-4-yl)-1H-benzo[d]imidazol-1-yl)(pyridin-4-yl)methanone (39)

Yellow powder, yield: 71%. M. p: 186 - 187 °C, ¹H NMR (DMSO-*d*₆, 400 MHz) δ: 2.35 (s, 3H); 7.29 - 7.31 (m, 2H); 7.37 - 7.39 (m, 3H); 7.42 - 7.55 (m, 9H); 7.80 (d, *J* = 5.2, 2H); 7.86 (d, *J* = 5.2, 1H); 8.87 (s, 1H). ESI-MS: 455.52 (C₂₉H₂₁N₅O, [M+H]⁺).

4.6. Minimum inhibitory concentration (MIC) assay using TTC double dilution method

The MTT is defined as the lowest concentration of the substance that prevents visible bacterial growth. Two Gram-negative bacterial strains: *E. coli* ATCC 25922 and *P. aeruginosa* ATCC 27853 and two Gram-positive bacterial strains: *B. subtilis* ATCC 530 and *S. aureus* ATCC 25923 were employed in the antibacterial activities

test, using the method recommended by National Committee for Clinical Laboratory Standards (NCCLS). By TTC double dilution method, the *in vitro* activities of the compounds were tested in nutrient broth (NB) for bacteria. Seeded broth (broth containing microbial spores) was prepared in NB from 24 h old bacterial cultures on nutrient agar (Hi-media) at 37 °C. The bacterial suspension was adjusted with sterile saline to a concentration of 1×10^4 to 1×10^5 CFU/mL. The tested compounds and reference drugs were prepared by two- fold serial dilution to obtain the required concentrations of 250, 125, 62.5, 31.25, 15.63, 7.81, 3.91, 1.95 $\mu\text{g/mL}$. The tubes were incubated in BOD incubators at 37 °C for bacteria. The MICs were recorded by visual observations after 24 h (for bacteria) of incubation. Antibiotic DDCP and kanamycin B were used as standards for bacterial. The observed MICs are presented in Table 3.

4.7. FabH inhibition activity

The potency of FabH inhibition (IC_{50}) was determined using [^3H]- or [^{14}C]-radiolabeled substrates (IC_{50} values correspond to the concentration at which half of the enzyme activity is inhibited by the compound). This was accomplished at fixed concentrations of acetyl-CoA in a coupled FabD/FabH assay system that generates the substrate malonyl-ACP *in situ*. Subsequently, the FabH acetylation reaction was performed to exclude the possible contribution of undesired FabD inhibitory activity. Compounds were included in cocrystallization trials with *Enterococcus faecalis* and *Haemophilus influenzae* FabH proteins and the derived protein-inhibitor cocrystal structures were used to further optimize the inhibitors. The FabH inhibition activity results are presented in Table 3.

4.8. Cytotoxicity test and Hemolysis test

The cytotoxic activity *in vitro* was measured against mammalian cells, human macrophage using the MTT assay. The cell was grown in DMEM medium supplemented with 10% FBS and 1 \times antimycotic and antibacterial solution (sigma USA) at 37 °C, in humidified atmosphere having 5% CO_2 . 100 μL of the confluent fibroblast stock suspension was dispensed in 96-well tissue culture plate. The original medium from the wells was replaced with 100 μL serum free DMEM when the cells reached 90% confluence after 5 h incubation in a CO_2 incubator. Various concentrations of the compounds were added to the growing cells and incubated for

24 h. The absorbance was measured at a wavelength of 570 nm (OD570 nm) on an ELISA microplate reader. Three replicate wells were used for each concentration and each assay was measured three times, after which the average of CC_{50} was calculated. The cytotoxicity of each compound was expressed as the concentration of compound that reduced cell viability to 50% (CC_{50}).

Hemolytic activity was assayed using fresh capillary human blood. Erythrocytes were collected by centrifuging the blood three times in chilled phosphate buffered saline (PBS at 4 °C) at $1000 \times g$ for 10 min. The final pellet was resuspended in PBS to give a 2% w/v solution. Using a microtitre plate, 100 μ L of the erythrocyte solution was added to dextran, PLL, stearyl-PLL or stearyl-PLL + LDL (1-1000/mg/mL) in a volume of 100 μ L. Samples were then incubated for 3 h and the microtitre plate was centrifuged then at $1000 \times g$ for 10 min and the supernatants (100 μ L) transferred into a new microtitre plate. Hemoglobin release was determined spectrophotometrically using a microtitre plate reader (absorbance at 550 nm). Results were expressed as the amount of released hemoglobin induced by the compounds as a percentage of the total.

4.9. Protocol of ADMET study

The three-dimensional structures of the aforementioned compounds were constructed using Chem. 3D ultra 15.0 software [Chemical Structure Drawing Standard; Cambridge Soft corporation, USA (2016)]. Then they were minimized a CHARMM based force field the same as in docking study. The ADMET study was conducted using the Calculate Molecular Properties in Small Molecules module of the Discovery Studio (version 3.5). The ADMET properties map and data were provided by the ADMET Descriptors tool.

4.8 Experimental protocol for docking study

Molecular docking was carried out using the Discovery Studio (version 3.5) as implemented through the graphical user interface DS-CDOCKER protocol. The three-dimensional structures of the aforementioned compounds were constructed using Chem. 3D ultra 15.0 software [Chemical Structure Drawing Standard; Cambridge Soft corporation, USA (2016)], then they were energetically minimized by using MMFF94 with 5000 iterations and minimum RMS gradient of 0.10. The crystal structures of protein complex were retrieved from the RCSB Protein Data Bank ([http:// www.rcsb.org/pdb/home/home.do](http://www.rcsb.org/pdb/home/home.do)). All bound water and ligands were

eliminated from the protein. The molecular docking in this study was performed by inserting compound 31 into the binding pocket of *E. coli* FabH (PDB code: 1HNJ) based on the binding mode. Types of interactions of the docked protein with ligand-based pharmacophore model were analyzed after the end of molecular docking.

Acknowledgments

This work was supported by National Key R&D Program of China (SQ2017YFNC060022-05, 2017YFC0506005) and China Postdoctoral Science Foundation funded project (No. 2018M641927).

References

1. Otvos JL, Wade JD, Lin F et al. Designer antibacterial peptides kill fluoroquinolone-resistant clinical isolates. *Journal of Medicinal Chemistry* 2005; **48**: 5349-5359.
2. Li ZL, Li QS, Zhang HJ et al. Design, synthesis and biological evaluation of urea derivatives from α -hydroxybenzylamines and phenylisocyanate as potential FabH inhibitors. *Bioorg Med Chem* 2011; **19**: 4413-4420.
3. Cui Y, Dang YY, Zhang S, Ji R. Syntheses and antibacterial activity of a series of 3-(pyridine-3-yl)-2-oxazolidinone. *European Journal of Medicinal Chemistry* 2005; **40**: 209-214.
4. Lee JY, Jeong KW, Shin S et al. Antimicrobial natural products as beta-ketoacyl-acyl carrier protein synthase III inhibitors. *Bioorganic & Medicinal Chemistry* 2009; **17**: 5408-5413.
5. HJ Z, ZL L, HL Z. Advances in the research of β -ketoacyl-ACP synthase III (FabH) inhibitors. *Current Medicinal Chemistry* 2009; **19**: 1225-1237.
6. Clough RC, Matthis AL, Barnum SR, Jaworski JG. Purification and characterization of 3-ketoacyl-acyl carrier protein synthase III from spinach. A condensing enzyme utilizing acetyl-coenzyme A to initiate fatty acid synthesis. *Journal of Biological Chemistry* 1992; **267**: 20992-20998.

7. Khandekar SS, Daines RA, Lonsdale JT. Bacterial beta-ketoacyl-acyl carrier protein synthases as targets for antibacterial agents. *Current Protein & Peptide Science* 2003; **4**: 21-29.
8. Heath RJ, Rock CO. The Claisen Condensation in Biology. *Natural Product Reports* 2002; **19**: 581-596.
9. Heath RJ, Rock CO. Inhibition of beta-ketoacyl-acyl carrier protein synthase III (FabH) by acyl-acyl carrier protein in *Escherichia coli*. *Journal of Biological Chemistry* 1996; **271**: 10996-11000.
10. Shi L, Fang RQ, Zhu ZW et al. Design and synthesis of potent inhibitors of β -ketoacyl-acyl carrier protein synthase III (FabH) as potential antibacterial agents. *European Journal of Medicinal Chemistry* 2010; **45**: 4358-4364.
11. Jun W, Stephen M S, Katherine Y et al. Platensimycin is a selective FabF inhibitor with potent antibiotic properties. *Nature* 2006; **441**: 358-361.
12. Young K, Jayasuriya H, Ondeyka JG et al. Discovery of FabH/FabF inhibitors from natural products. *Antimicrob Agents Chemother* 2006; **50**: 519-526.
13. Zhang C, Ondeyka J, Herath K et al. Platensimycin and platencin congeners from *Streptomyces platensis*. *Journal of Natural Products* 2011; **74**: 329-340.
14. Allahverdiyev AM, Bagirova M, Abamor ES et al. The use of platensimycin and platencin to fight antibiotic resistance. *Infection & Drug Resistance* 2013; **6**: 99-114.
15. Evan M, Demain AL. Platensimycin and platencin: promising antibiotics for future application in human medicine. *Journal of Antibiotics* 2011; **64**: 705-710.
16. Musayev F, Sachdeva S, Scarsdale JN et al. Crystal structure of a substrate complex of *Mycobacterium tuberculosis* beta-ketoacyl-acyl carrier protein synthase III (FabH) with lauroyl-coenzyme A. *Journal of Molecular Biology* 2005; **346**: 1313-1321.
17. Jones PB, Parrish NM, Houston TA et al. A new class of antituberculosis agents. *Journal of Medicinal Chemistry* 2000; **43**: 3304-3314.
18. Mckinney DC, Eyermann CJ, Gu RF et al. Antibacterial FabH Inhibitors with Mode of Action Validated in *Haemophilus influenzae* by in Vitro Resistance Mutation Mapping. *Acs Infectious Diseases* 2016; **2**: 456-464.

19. Li P. Drug design and the mechanism of β -ketoacyl-acyl carrier protein synthase III (FabH) inhibitors; 2017.
20. Choudhari PB, Subramani PP, Khare SV et al. Investigation on quantitative structure activity relationships of benzoylamino benzoic acid derivatives as β -ketoacyl-acyl carrier protein synthase III (FabH) Inhibitors. *Marmara Pharmaceutical Journal* 2017; **21**: 631-643.
21. Ranjith PK, Rajeesh P, Haridas KR et al. Design and synthesis of positional isomers of 5 and 6-bromo-1-[(phenyl)sulfonyl]-2-[(4-nitrophenoxy)methyl]-1H -benzimidazoles as possible antimicrobial and antitubercular agents. *Bioorganic & Medicinal Chemistry Letters* 2013; **23**: 5228-5234.
22. Zhou B, Li B, Yi W et al. Synthesis, antioxidant, and antimicrobial evaluation of some 2-arylbenzimidazole derivatives. *Bioorganic & Medicinal Chemistry Letters* 2013; **23**: 3759-3763.
23. Elie CR, David G, Schmitzer AR. Strong antibacterial properties of anion transporters: a result of depolarization and weakening of the bacterial membrane. *Journal of Medicinal Chemistry* 2015; **58**: 2358-2366.
24. Braccio MD, Grossi G, Signorello MG et al. Synthesis, invitro antiplatelet activity and molecular modelling studies of 10-substituted 2-(1-piperazinyl)pyrimido[1,2- a]benzimidazol-4(10 H)-ones. *European Journal of Medicinal Chemistry* 2013; **62**: 564-578.
25. Xin-Mei P, Gui-Xin C, Cheng-He Z. Recent developments inazole compounds as antibacterial and antifungal agents. *Current Topics in Medicinal Chemistry* 2013; **13**: 1963-2010.
26. Zhou C, Kegui YU, Meng J et al. Dibenzimidazole and onium compound thereof, preparation method and medical use thereof. CN Patent, 2009.
27. Lan R, Liu Q, Fan P et al. Structure-activity relationships of pyrazole derivatives as cannabinoid receptor antagonists. *Journal of Medicinal Chemistry* 1999; **42**: 769-776.
28. Norinder U, Bergström CAS. Prediction of ADMET Properties. *Chemmedchem* 2006; **1**: 920-937.
29. Gleeson MP. Generation of a set of simple, interpretable ADMET rules of thumb. *Journal of Medicinal Chemistry* 2008; **51**: 817-834.

30. Egan WJ. Prediction of intestinal permeability. *Advanced Drug Delivery Reviews* 2002; **54**: 273-289.
31. Liu J, Wang F, Ma Z et al. Structural Determination of Three Different Series of Compounds as Hsp90 Inhibitors Using 3D-QSAR Modeling, Molecular Docking and Molecular Dynamics Methods. *International Journal of Molecular Sciences* 2011; **12**: 946-970.
32. Parmar KC, Vora JJ, Vasava SB. Synthesis, spectral and microbial studies of some novel schiff base derivatives of 2-amino pyridine. *Journal of Chemical and Pharmaceutical Research* 2014, **6**: 1259-1263.
33. Rathelot P, Azas N, El-Kashef H et al. 1,3-diphenylpyrazoles: synthesis and antiparasitic activities of azomethine derivatives. *European Journal of Medicinal Chemistry* 2002; **37**: 671-679.
34. Kumar S, Ceruso M, Tuccinardi T et al. Pyrazolylbenzo[*d*]imidazoles as new potent and selective inhibitors of carbonic anhydrase isoforms Hca IX and XII. *Bioorganic & Medicinal Chemistry* 2016; **24**: 2907-2913.

- > 27 novel Pyrazol-Benzimidazole amide derivatives have been synthesized, and their biological activities were evaluated as potential FabH inhibitors.
- > Cytotoxicity, hemolytic activities and *in silico* ADMET were also appraised as well as molecular docking.
- > Compound **31** showed the most potent inhibitory activity against four tested bacterial and FabH.
- > Crystal structure of compound **17** was determined.

ACCEPTED MANUSCRIPT